Letter

# Thermoelectric transport properties of gapless pinned charge density waves

Tomas Andrade [1] and Alexander Krikun [2,*]

[1] *Departament de Física Quàntica i Astrofísica, Institut de Ciències del Cosmos, Universitat de Barcelona, Martí i Franquès 1, E-08028 Barcelona, Spain*

[2] *Nordita, KTH Royal Institute of Technology and Stockholm University, Hannes Alfvéns väg 12, SE-106 91 Stockholm, Sweden*

(Received 4 April 2022; revised 6 July 2022; accepted 11 July 2022; published 29 July 2022)

Quantum strongly correlated matter exhibits properties which are not easily explainable in the conventional framework of Fermi liquids. Universal effective field theory tools are applicable in these cases regardless of the microscopic details of the quantum system, since they are based on symmetries. It is necessary, however, to construct these effective tools in full generality, avoiding restrictions coming from particular microscopic descriptions which may inadequately constrain the coefficients that enter in the effective theory. In this work we demonstrate with explicit examples how the hydrodynamic coefficients, which have been recently reinstated in the effective theory of pinned charge density waves (CDWs), can affect the phenomenology of the thermoelectric transport in strongly correlated quantum matter. Our examples, based on two classes of holographic models with pinned CDW, have microscopics which are conceptually different from Fermi liquids. Therefore, the above transport coefficients are nonzero, contrary to the conventional approach. We show how these coefficients allow one to take into account the change of sign of the Seebeck coefficient and the low resistivity of the CDW phase of the cuprate high temperature superconductors, without referring to the effects of Fermi surface reconstruction.

DOI: 10.1103/PhysRevB.106.L041118

## I. INTRODUCTION

The transport properties of the charge density wave (CDW) ordered states of strongly correlated quantum matter, in particular in cuprate superconductors, attract a great deal of attention. The CDW plays an important role in the phase diagram of the cuprates: it appears as an order parameter in a subregion across the pseudogap and superconductor phases, as well as a fluctuation at higher temperatures in the strange metal phase [1]. It can be demonstrated [2] that the onset of CDW leaves an imprint on the thermopower (or Seebeck coefficient), which starts decreasing at the CDW critical temperature $T_{\text{CDW}}$ and reaches negative values at low $T$'s. This feature is observed in various compounds [3–8] and can be considered as a universal signature of CDW. From the point of view of the Fermi liquid theory, this behavior may be understood as a reconstruction of the Fermi surface [9], yet to be detected. However, the very applicability of the Fermi liquid to cuprates is debatable [10–12] and the need of alternative approaches to the physics of thermopower in these systems persists [13,14].

Irrespective of the microscopic description of a particular system, one can construct an effective theory (EFT) of its low energy properties by symmetry considerations [15]. For exact global symmetries, this procedure leads to hydrodynamics. If a global symmetry is spontaneously broken, the corresponding Goldstone mode appears in the spectrum and must be added to the hydrodynamic degrees of freedom. If the spontaneously broken symmetry is only approximate (there is a small explicit breaking source), the hydrodynamic description of massive pseudo-Goldstone mode can be developed [16–19]. The phases of matter with pinned CDW fall in the latter class: the spatial structure of CDW breaks translation symmetry spontaneously, while pinning provides an explicit symmetry breaking source.

The effective theory of broken translations has long been appreciated as a tool to address the dynamics of the CDW phases in quantum systems [20]. Recently, it has experienced a renaissance motivated in part by the appearance of a class of physical models described by the holographic duality [21,22]. These models, on one hand, can exhibit the CDW phases [23–26] (see [27] for recent review) and therefore must be describable by a symmetry based EFT. On the other hand, they defy the principles of gapped Fermi liquid used in the earlier EFT constructions to constrain certain hydrodynamic coefficients. Therefore, the need to relax some of these constraints has been identified recently, leading to a new generation of EFTs, with an enlarged set of nonzero hydrodynamic coefficients: the Galilean symmetry constraints have been relaxed in [16–18], the effects of pinning where included in [16–19], and the effects of background strain have been addressed in [28,29].

Here we study explicit examples of translational symmetry breaking in holographic models. We evaluate all AC and DC conductivities and match the results with the EFT description

*Corresponding author: krikun@nordita.org

of [18,19,29]. We show that the transport coefficients, namely, the incoherent conductivity and Goldstone mode diffusivity, are nonzero in the considered examples and lead to alternative phenomenology: the change of sign of the Seebeck coefficient discussed above, and the absence of an exponential gap in the resistivity of the symmetry broken state. The latter is also a feature of the CDW phase of cuprates [30–33].

In the following section we review the hydrodynamic EFT of pinned CDWs. Then, we construct the holographic dual to a quantum system with CDW order and show that its AC conductivity, as expected, is very well described by the EFT, albeit with parameters which do not follow the conventional Fermi liquid logic. We obtain the DC conductivities and demonstrate some phenomenological features, which may be studied experimentally. The extra details are summarized in the Supplemental Material [34] (see also, Refs. [35,36] therein).

## II. EFFECTIVE THEORY OF CHARGE DENSITY WAVES

In a hydrodynamic approach, the effective theory of pinned CDW can be built using exclusively the symmetry considerations [16,17,19,28,29,37], and, importantly, is valid irrespective of whether or not the quantum system admits a perturbative treatment. Thus, EFT forms a convenient basis for the analysis of various experimental measurements, representing all data in terms of a limited number of hydrodynamic coefficients.

We will rely on the effective theory description of CDW developed in [28,29,38]. Let us restrict the model of [29] to a space-time with two spatial dimensions $(x, y)$, with a unidirectional spontaneous spatial structure: CDW. Introducing an intrinsic coordinate $\phi$ along the CDW, one can characterize its embedding in space by a single "crystal field" $\phi(x, y)$. The ground state (a homogeneous CDW with no defects) corresponds to $\phi_0(x, y) = \alpha x$.[1] Note that the translation of the CDW as a whole, the sliding mode, is encoded in the shifts of $\phi$: $\phi \to \phi + \delta\phi$. Therefore one readily identifies $\phi$ as a Goldstone field.

We restrict our attention to small low-frequency, long-wavelength fluctuations of the CDW structure $\phi = \phi_0 + \alpha\delta\phi(t, x)$, the local chemical potential $\mu = \mu_0 + \delta\mu(t, x)$ and temperature $T = T_0 + \delta T(t, x)$, and local velocity field $u^\mu = \{1, 0, 0\} + \delta u^\mu(t, x)$. To compute the two-point functions relevant for transport, we consider external sources for the current and energy-momentum tensor: the electric field $\delta\partial_t A_x(t, x)$ and the background metric perturbation $\delta g_{tx}(t, x)$. Moreover, we take into account the effect of the crystal lattice, which simultaneously breaks translations explicitly, introducing a finite momentum dissipation $\Gamma$, and pins the CDW, providing a mass $m_\phi^2$ to the Goldstone mode. As long as $\Gamma$ and $m_\phi^2$ are small, this "weak pinning" effect can be treated as a small correction to the hydrodynamic conservation laws. The pinning leads to a finite lifetime of the Goldstone, parametrized by the phase relaxation term $\Omega$ [16–19,37–39]. The full set of hydrodynamic constitutive relations, resulting from the framework of [29], is listed in Supplemental Material [34] Sec. A. Here we assume Lorentz symmetry [40], and the expression for the electric current and the Goldstone configuration equation (Josephson relation) read[2]

$$J^x = \rho\delta u^x + \gamma(\partial_t\delta\phi - \delta u^x) - \sigma_q\Big(T_0\partial_x\frac{\mu}{T} + \partial_t\delta A_x\Big), \quad (1)$$

$$\partial_t\delta\phi - \delta u^x - \frac{B+G}{\sigma_\phi}\partial_x^2\delta\phi - \frac{\gamma'}{\sigma_\phi}\Big(T_0\partial_x\frac{\mu}{T} + \partial_t\delta A_x\Big) = -\Omega\delta\phi. \quad (2)$$

In addition, we quote the stress-energy and current conservation laws, modified by the explicit sources and symmetry breaking terms:

$$\nabla_\mu T^\mu_t = 0, \qquad \nabla_\mu J^\mu = 0, \quad (3)$$

$$\nabla_\mu T^\mu_x = -\rho\partial_t\delta A_x + \Gamma T_{tx} - G m_\phi^2\delta\phi. \quad (4)$$

Here $\nabla_\mu$ is a covariant derivative constructed with the perturbed metric, $\{P, \rho, s\}$ are thermodynamic pressure, charge density, and entropy in the ground state, $\{B, G\}$ are bulk and shear elastic moduli of the spontaneous structure, $\{\zeta, \eta\}$ are bulk and shear viscosities, while $\{\sigma_q, \gamma, \gamma', \sigma_\phi\}$ are four more hydrodynamic coefficients which we discuss now in more detail.

The $\sigma_q$ and $\sigma_\phi^{-1}$ coefficients are usually set to zero in the standard treatment of CDW in gapped quantum systems [20]. If we examine the Josephson relation in the absence of perturbative sources and pinning, we see that at any finite momentum $k$ the Goldstone mode decays with the rate $\sigma_\phi^{-1}(B+G)k^2$, therefore $\sigma_\phi^{-1}$ controls the Goldstone diffusivity [26,42]. However, in a gapped quantum system, the Goldstone mode cannot decay even at finite momentum, unless the momentum is large enough to cross the gap. Therefore, at zero temperature one sets $\sigma_\phi^{-1} = 0$ and all terms except $\delta u_x$ drop out from (2). On the other hand, at finite temperature one expects $\sigma_\phi^{-1}$ to be exponentially suppressed by the scale of the gap.

The other unusual coefficient is $\sigma_q$. This is allowed from the EFT perspective, but it is absent in systems where transport is mediated by quasiparticles and the current is constrained by Galilean symmetry $J^x = \rho\delta u^x$. This coefficient is related to "incoherent conductivity," which has been discussed extensively in connection to holographic models [23–26,43–46] and plays a crucial role here.

We can plug in the constitutive relations into the conservation laws and solve the system of differential equations with respect to hydrodynamic variables $\{\delta u^x, \delta\mu, \delta T, \delta\phi\}$ in the presence of external sources $\{\delta A_x, \delta g_{tx}\}$. Inserting the solutions back into the constitutive relations, we obtain the expectation values for various operators in terms of perturbative sources [40]. This allows us to evaluate the two-point functions $\langle J^x J^x\rangle$, $\langle J^x T^{tx}\rangle$, $\langle T^{tx} J^x\rangle$, and $\langle T^{tx} T^{tx}\rangle$. As one can

[1] $\alpha$ characterizes the "wavelength" of the CDW; however, it is arbitrary given the reparametrization freedom of $\phi$.

[2] In [29,41] the extra thermodynamic quantity "lattice pressure" plays a significant role in the model, but it is irrelevant here (see Supplemental Material [34] Sec. A).

show from locality of the hydrodynamic equations [18], positivity of entropy production [19], or the Onsager relation between $\langle J^x T^{tx}\rangle$ and $\langle T^{tx} J^x\rangle$ (see Supplemental Material [34] Sec. A), the coefficients are related as [26,37,38,42,47–51]

$$\gamma' = -\gamma, \qquad \Omega = \sigma_\phi^{-1} m_\phi^2 G. \tag{5}$$

Recalling the definition of the heat current in the presence of a chemical potential [52], $Q^x = J^x + \mu T^{tx}$, we arrive at the full matrix of AC thermoelectric conductivities [53] ($\bar\kappa$ is thermal conductivity at zero bias),

$$\begin{pmatrix} J^x \\ Q^x \end{pmatrix} = \begin{pmatrix} \sigma & T\alpha \\ T\bar\alpha & T\bar\kappa \end{pmatrix} \begin{pmatrix} E_x \\ -\frac{\partial_x T}{T} \end{pmatrix}. \tag{6}$$

At the zero wavelength limit

$$\begin{aligned}
\sigma(\omega) &= \sigma_0 + \frac{\tilde\rho^2(\Omega - i\omega) - \tilde\gamma^2\omega_0^2(\Gamma - i\omega) - 2\tilde\rho\tilde\gamma\omega_0^2}{\mu_0^2\chi_{\pi\pi}\big((\Gamma - i\omega)(\Omega - i\omega) + \omega_0^2\big)},\\
\frac{T}{\mu_0}\alpha(\omega) &= -\sigma_0 \\
&\quad + \frac{\tilde\rho\tilde s(\Omega - i\omega) + \tilde\gamma^2\omega_0^2(\Gamma - i\omega) - (\tilde s - \tilde\rho)\tilde\gamma\omega_0^2}{\mu_0^2\chi_{\pi\pi}\big((\Gamma - i\omega)(\Omega - i\omega) + \omega_0^2\big)},\\
\frac{T}{\mu_0^2}\bar\kappa(\omega) &= \sigma_0 + \frac{\tilde s^2(\Omega - i\omega) - \tilde\gamma^2\omega_0^2(\Gamma - i\omega) + 2\tilde s\tilde\gamma\omega_0^2}{\mu_0^2\chi_{\pi\pi}\big((\Gamma - i\omega)(\Omega - i\omega) + \omega_0^2\big)},
\end{aligned} \tag{7}$$

where

$$\begin{aligned}
&\sigma_0 = \sigma_q + \frac{\gamma^2}{\sigma_\phi}, \quad \tilde\rho = \mu_0\rho, \quad \tilde s = T_0 s, \quad \chi_{\pi\pi} = \tilde\rho + \tilde s,\\
&\tilde\gamma = \mu_0\chi_{\pi\pi}\gamma/\sigma_\phi, \quad \omega_0^2 = G m_\phi^2/\chi_{\pi\pi}.
\end{aligned} \tag{8}$$

In the ordered state far from $T_c$ ($\omega_0 \gtrsim \Omega, \Gamma$) these expressions correspond to the peak in the real part of the spectra, located at finite "pinning frequency" $\omega_0$ with width $(\Omega + \Gamma)$. This is a manifestation of the gapped coherent sliding mode. The DC conductivities display a mixture of coherent and incoherent contributions, which can be recast as

$$\begin{aligned}
\sigma &= \sigma_q + \sigma_\phi^{-1}\frac{(\rho - \gamma)^2}{1 + \frac{\Gamma\chi_{\pi\pi}}{\sigma_\phi}}, \quad \frac{\bar\kappa T}{\mu^2} = \sigma_q + \sigma_\phi^{-1}\frac{\left(\frac{sT}{\mu} + \gamma\right)^2}{1 + \frac{\Gamma\chi_{\pi\pi}}{\sigma_\phi}},\\
\frac{\alpha T}{\mu} &= -\sigma_q + \sigma_\phi^{-1}\frac{(\rho - \gamma)\left(\frac{sT}{\mu} + \gamma\right)}{1 + \frac{\Gamma\chi_{\pi\pi}}{\sigma_\phi}}.
\end{aligned} \tag{9}$$

These expressions represent the main outcome of the EFT [18,28,37] which we are going to study. Note that both terms are usually negligible in the conventional gapped CDW: $\sigma_q$ is zero because of Galilean invariance, while $\sigma_\phi^{-1}$ is exponentially suppressed due to a gap in the spectrum.

In presence of finite $\sigma_q$ and $\sigma_\phi^{-1}$, however, the DC conductivities depart from the conventional picture. First, the electric conductivity is finite even in the broken phase, and second, the sign of the thermopower $\alpha$ is a result of the interplay between $\sigma_q$ and $\sigma_\phi^{-1}$ terms. In what follows we explore how these mechanisms come about in non-Fermi liquid, holographic models.

### III. HOLOGRAPHIC MODEL OF GAPLESS CDW

The essence of holographic modeling is the correspondence between strongly correlated quantum systems and classical black holes in auxiliary space-times, which are constructed according to a rigorous set of rules: the "holographic dictionary" [21,22,52,53]. In this paradigm, the quantum system at finite temperature $T$ and chemical potential $\mu$ in a 2+1 dimensional space-time corresponds to a black hole in a 3+1 dimensional curved space-time, whose horizon radius and charge are set by $T$ and $\mu$. The crystal lattice can be introduced via periodic modulation of the chemical potential [54–60]: $\mu(x) = \mu_0[1 + A\cos(kx)]$.[3] We will consider a model with small $A = 0.04$, describing the weakly pinned CDW. The spontaneous structure formation is realized as an instability of the black hole against formation of the spatially modulated "hair" [61–63]. The interplay between the explicit and spontaneous translation symmetry breaking has been studied extensively in this setup [39,64–66] (note also other approaches [26,27,42,47–49,67–76]; see Suplementary Material Sec. D). The action of the model reads

$$\begin{aligned}
S = &\int d^4x\sqrt{-g}\left(R - 2\Lambda - \frac{1}{2}(\partial\psi)^2 - \frac{\tau(\psi)}{4}F^2 - W(\psi)\right)\\
&- \frac{1}{2}\int \theta(\psi) F\wedge F.
\end{aligned} \tag{10}$$

where $F = dA$ is the field strength of the $U(1)$ gauge field dual to a $U(1)$ global charge, and $\psi$ is an axion field in the bulk coupled to the $\theta$ term, which drives a CDW instability. $R$ and $\Lambda$ are the Ricci curvature and negative cosmological constant, which govern the structure of asymptotically anti–de Sitter (AdS) space in the bulk. The qualitative features we reveal depend only mildly on the precise form of the potentials

$$\begin{aligned}
&\tau(\psi) = 1 + \cdots, \quad W(\psi) = -\psi^2 + \cdots,\\
&\theta(\psi) = \frac{c_1}{2\sqrt{6}}\psi + \cdots;
\end{aligned} \tag{11}$$

for more details see Supplemental Material [34] Sec. B.

The holographic dictionary identifies the asymptotics of the gauge field profile near the AdS boundary (located at radial coordinate $z \to 0$) with the chemical potential and $U(1)$ charge density: $A_t(x,z)|_{z\to 0} = \mu(x)z + \rho(x)z^2$. Given the classical solution to the Einstein equations following from (10) with appropriate boundary conditions set by $\mu(x)$ and $T$, one can compute the charge density profile $\rho(x)$ and observe formation of spontaneous CDWs below a certain critical temperature $T = T_0(c_1)$. As the temperature is lowered, the order parameter—the amplitude of the charge density modulation—grows and the effective theory of pinned CDWs is applicable. One can achieve a similar behavior by tuning the coupling constant $c_1$ at fixed temperature.

To evaluate the AC conductivities, we introduce perturbative sources for the electric current and stress-energy tensor, encoded in the near-boundary asymptotes of the gauge field $A_x(z)$ and metric $g_{tx}(z)$. After solving the equations of motion,

[3] This unidirectional crystal model allows us to simplify the treatment, preserving all the necessary physics.

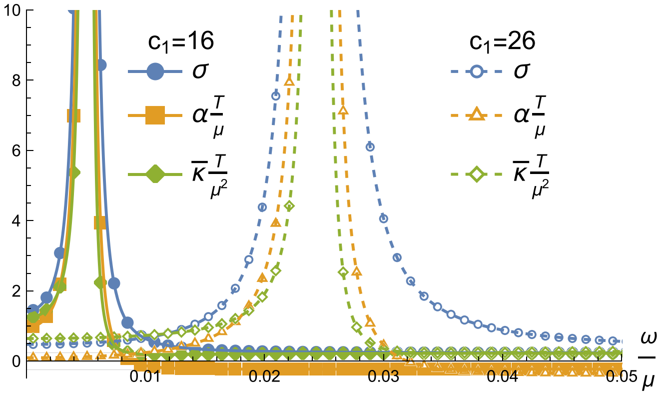


FIG. 1. The pinned peak in AC conductivities. The filled dots and solid lines show the AC data for the conductivities in the holographic model with $c_1 = 16$ and the fits with (7). The empty dots and dashed lines show the same with $c_1 = 26$. Data were taken for the 2/1 commensurate states with $T/\mu = 0.1,\ k/\mu \approx 2.1,\ A = 0.04$.

we read off the subleading components and take the variations with respect to the sources. We thus obtain the two-point functions $\langle J^x J^x\rangle$, $\langle J^x T^{tx}\rangle$, $\langle T^{tx} J^x\rangle$, and $\langle T^{tx} T^{tx}\rangle$ from which we read all AC thermoelectric conductivities (6). The numerical calculations are demanding, especially at low temperatures. To circumvent this, we fix the temperature and tune the coupling $c_1$ to control the order parameter; see Supplemental Material [34] Sec. B for details.

In the weak pinning regime ($A = 0.04$), the results have precisely the shape predicted by the effective theory; see Fig. 1: the peak located at finite frequency $\omega_0$. As we discuss in Supplemental Material [34] Sec. C, we perform a set of cross-checks of the model expressions (1). First, we obtain the same values of hydrodynamic coefficients when independently fitting $\sigma$, $\alpha$, and $\bar{\kappa}$. Moreover, we extract thermodynamic data from the AC linear response fits, which agree with the data obtained as the operator expectation values in the ground state of the model. This check also shows that the extra thermodynamic quantities, discussed in [19,28,28,41], such as the lattice pressure, can be safely neglected. Finally, we get excellent agreement between the DC conductivities, obtained by the expressions (9) using the values of the hydrodynamic coefficients from the AC fits, and the DC transport properties evaluated using the near horizon data in the holographic

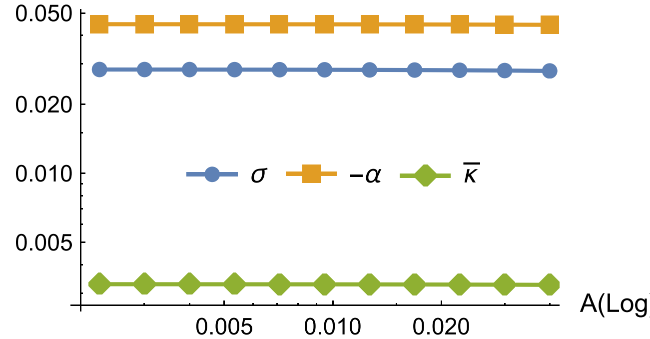


FIG. 3. Dependence of the DC thermoelectric conductivities on the pinning scale $A$. The data were taken for the 2/1 commensurate states with $k/\mu = 2, A = 0.04$.

ground state, as we discuss in a moment. These checks support the statement that the effective theory of pinned CDW from Sec. II describes well the holographic results.

## IV. DC TRANSPORT

The DC transport of the holographic model can be studied with greater precision than the AC conductivities since it can be extracted from near horizon data of the background geometry [25,58,77–81].

The results for temperature series of solutions with different $c_1$ couplings are shown in Fig. 2. One can recognize the unconventional behavior of the electric conductivity, which decreases at small temperature as a certain power law, instead of the activated exponential behavior [$\sim \exp(-\Delta_{CDW}/T)$] expected for the gapped CDW. Moreover the thermopower changes sign at a certain temperature, which depends on the coupling $c_1$. While it is unusual in the conventional treatment, this behavior can be well incorporated in the generalized EFT framework, Sec. II. Note also that, as we show in Fig. 3, the DC conductivities are insensitive to the scale of the explicit symmetry breaking (crystal lattice or impurities ), which supports our treatment of $\Gamma$ as a small parameter in (9).

In the previous section we established the validity of EFT as we vary the order parameter dialing $c_1$. Assuming that EFT continues to be applicable in the regimes where the order grows due to the decrease of temperature, we can use (9) and extract all the hydrodynamic coefficients, having the DC conductivities at hand (in the weak pinning regime). This leads to

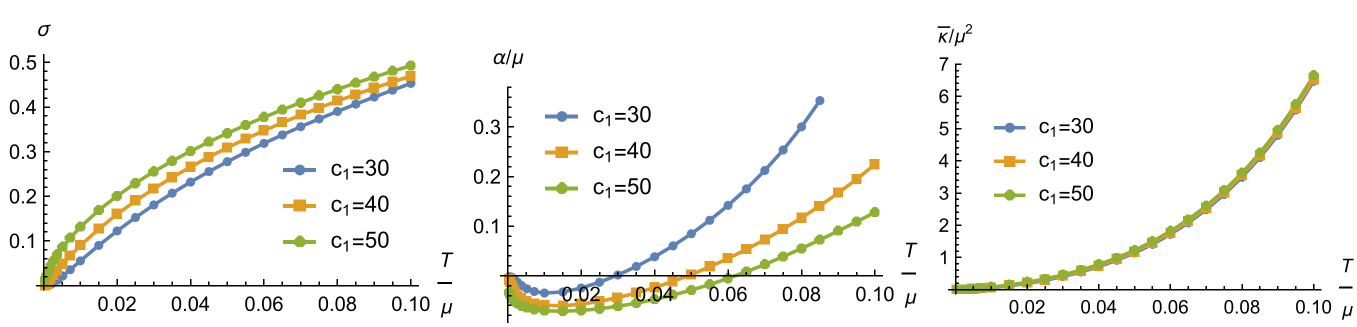


FIG. 2. The evolution DC thermoelectric conductivities at small temperatures. The holographic model with different values of the coupling $c_1$ is considered. Note that thermopower changes sign at some coupling-dependent point. Data were taken for the 2/1 commensurate states with $k/\mu = 2, A = 0.04$.

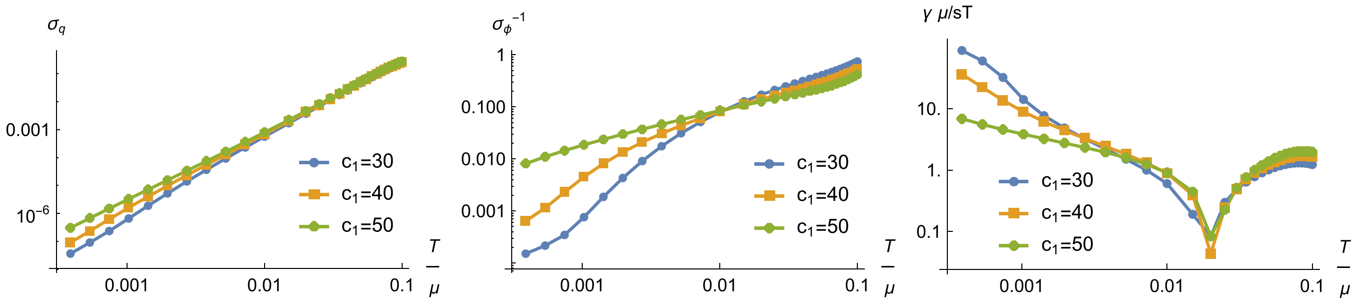


FIG. 4. The behavior of effective theory parameters at low temperatures. Plots have log-log scales. Incoherent conductivity $\sigma_q$ and Goldstone diffusivity behave as certain power laws, but the former does not depend on the coupling $c_1$. $\gamma$ changes sign at some $T/\mu \approx 0.02$ for all $c_1$. Note that this is not related to the change of sign in $\alpha$. $\gamma\mu/sT$ does not quite saturate at 1, as suggested in [26,42]. Data are the as in Fig. 3.

the results shown in Fig. 4. We see that the EFT parameters $\sigma_q$ and $\sigma_\phi^{-1}$ are indeed nonzero and behave as power laws rather then as gapped exponentials.

The relative contributions of the various terms in (9) to the DC transport are shown in Fig. 5. Interestingly, we see that the electric conductivity is dominated by the $\sigma_\phi^{-1}\rho^2$ term, while the heat conductivity ($\bar{\kappa}$ and, as we checked, $\kappa = \bar{\kappa} - \alpha^2/\sigma$) is controlled by $\sigma_q$. This means that the behaviors of the electric and heat conductivities are not related to each other at the level of EFT, and the Wiedemann–Franz law ($\kappa/\sigma \sim T$) may not arise in materials with these "gapless pinned CDWs." Looking at the thermopower, we see that the two terms in (9) are of the same order and approximately cancel each other. This cancellation is the reason for the sign change in $\alpha$, as seen on Fig. 2. Therefore, the exact temperature where the sign changes depends on subleading contributions, and does not point to some qualitative change, as it would for Fermi surface reconstruction.

The phenomenological features which we observe here are not specific to a particular holographic model. As we show in Supplemental Material [34] Sec. D, we obtain similar results in a different setup based on a helical lattice. The universal feature, which appears in both cases, is the absence of exponential suppression of either $\sigma_q$ or $\sigma_\phi^{-1}$, leading to a nontrivial interplay between the terms in (9). The remarkable cancellation of terms in $\alpha$ as well as the exchange of dominance of the $\sigma_q$ and $\sigma_\phi^{-1}$ terms in $\sigma$ and $\bar{\kappa}$ are also persistent features in our data. This might point out some universal relation between $\gamma\sigma_\phi^{-1}$ and $\sigma_q$ as suggested in [26,42]; see Supplemental Material [34] Sec. E for the further discussion on this.

## V. CONCLUSION

In this Letter we demonstrate how the parameters in the effective theory of pinned charge density waves [16–19,28,29,38], which are absent in gapped quantum systems, can affect the thermoelectric transport when they are nonzero. The absence of a clean gap in the spectrum can be a result of the quantum continuum being present in the system. The effects of such a continuum spectrum have been studied in relation to the physics of plasmons [82], the dynamics of pattern formation [39], and fermion spectral functions [83–85].

In explicit examples constructed by means of holographic duality, we show that the "gapless" pinned charge density waves demonstrate nonvanishing conductivity in the pinned CDW phase, change of sign in the thermopower (unrelated to the reconstruction of the Fermi surface), the conceptual absence of the Wiedemann-Franz law, and low sensitivity of the transport properties to the concentration of impurities. All these phenomenological features are observed in the underdoped phases of cuprate high temperature superconductors, where charge density waves are present.

We hope that these examples will encourage the use of the improved EFT in the analysis of the transport experiments in CDW cuprates, which in turn could clarify their physical nature and, perhaps, would unveil the properties of the underlying quantum criticality.

We also point out that the phenomenology of the DC transport, described above, being a consequence of the pinned CDW behavior, predicts the specific shapes of the spectra of AC conductivities (7), which makes the experiments on the optical spectroscopy particularly important.

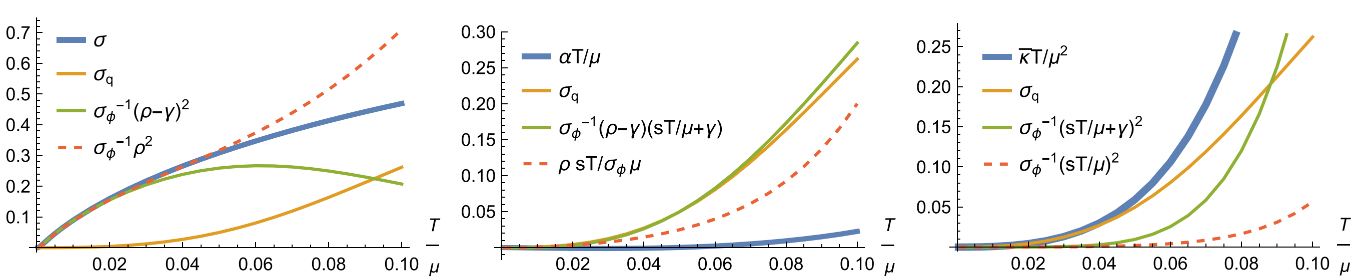


FIG. 5. The contributions to DC conductivities from various terms in (9). At low $T$ electric conductivity is dominated by the $\sigma_\phi^{-1}$ term, heat conductivity is dominated by the $\sigma_q$ term, while thermopower is a result of a fine balance between them. Red lines assume $\gamma = 0$ and help to one appreciate the role of $\gamma$. Data are as in Fig. 3 for $c_1 = 40$.

It is worth mentioning that, when deriving the expressions (9) and (7) and focusing on the qualitative effects, we omitted other hydrodynamic coefficients, pointed out in [19], which play a subleading role in our discussion. One should keep this in mind when performing precision tests of (9) and (7).

Finally, we point out that the considered EFT framework is based on the Lorentz symmetry and therefore the "incoherent contributions" $\sim\sigma_q$ in all the conductivities (9) are related. In the absence of Lorentz symmetry one allows instead three independent coefficients: $\sigma_q$, $\alpha_q$, and $\kappa_q$. A nonzero negative $\alpha_q$ of order $\sigma_q$ could lead to a similar cancellation phenomenon in thermopower.

## ACKNOWLEDGMENTS

We thank K. Schalm, J. Zaanen, and F. Balm for long lasting collaboration in this subject. We are grateful to J. Armas, A. Jain, A. Amoretti, D. Brattan, and B. Gouteraux for useful communication and valuable advice. A.K. thanks D. Popovic, F. Lombardi, R. Arpaia, U. Gran, and D. Marsh for insightful comments. A.K. acknowledges the hospitality of the physics department of Chalmers Technical University, where the preliminary results of this work were discussed. The work of A.K is supported by VR Starting Grant No. 2018-04542 of Swedish Research Council. The work of T.A. is supported in part by the ERC Advanced Grant No. GravBHs-692951 and by Grant No. CEX2019-000918-M funded by Ministerio de Ciencia e Innovación (MCIN) and Agencia Estatal de Investigación (AEI), 10.13039/501100011033. The numerical computations were enabled by resources provided by the Swedish National Infrastructure for Computing (SNIC), partially funded by the Swedish Research Council through Grant Agreement No. 2018-05973, at SNIC Science Cloud and PDC Center for High Performance Computing, KTH Royal Institute of Technology. Nordita is supported in part by Nordforsk.

[1] R. Arpaia and G. Ghiringhelli, Charge order at high temperature in cuprate superconductors, J. Phys. Soc. Jpn. **90**, 111005 (2021).

[2] C. Collignon, A. Ataei, A. Gourgout, S. Badoux, M. Lizaire, A. Legros, S. Licciardello, S. Wiedmann, J.-Q. Yan, J.-S. Zhou *et al.*, Thermopower across the phase diagram of the cuprate $La_{1.6-x}Nd_{0.4}Sr_xCuO_4$: Signatures of the pseudogap and charge density wave phases, Phys. Rev. B **103**, 155102 (2021).

[3] M. Hucker, V. Kataev, J. Pommer, O. Baberski, W. Schlabitz, and B. Büchner, Consequences of stripe order for the transport properties of rare earth doped $La_{2-x}Sr_xCuO_4$, J. Phys. Chem. Solids **59**, 1821 (1998).

[4] Y. Nakamura and S. Uchida, Anisotropic transport properties of single-crystal $La_{2-x-y}Nd_ySr_xCuO_4$: Effect of the structural phase transition, Phys. Rev. B **46**, 5841 (1992).

[5] Q. Li, M. Hücker, G. D. Gu, A. M. Tsvelik, and J. M. Tranquada, Two-Dimensional Superconducting Fluctuations in Stripe-Ordered $La_{1.875}Ba_{0.125}CuO_4$, Phys. Rev. Lett. **99**, 067001 (2007).

[6] J. Chang, R. Daou, C. Proust, D. LeBoeuf, N. Doiron-Leyraud, F. Laliberté, B. Pingault, B. Ramshaw, R. Liang, D. Bonn *et al.*, Nernst and Seebeck Coefficients of the Cuprate Superconductor $YBa_2Cu_3O_{6.67}$: A study of Fermi Surface Reconstruction, Phys. Rev. Lett. **104**, 057005 (2010).

[7] N. Doiron-Leyraud, S. Lepault, O. Cyr-Choiniere, B. Vignolle, G. Grissonnanche, F. Laliberté, J. Chang, N. Barišić, M. K. Chan, L. Ji *et al.*, Hall, Seebeck, and Nernst Coefficients of Underdoped $HgBa_2CuO_{4+\delta}$: Fermi-Surface Reconstruction in an Archetypal Cuprate Superconductor, Phys. Rev. X **3**, 021019 (2013).

[8] S. Badoux, S. A. A. Afshar, B. Michon, A. Ouellet, S. Fortier, D. LeBoeuf, T. P. Croft, C. Lester, S.M. Hayden, H. Takagi *et al.*, Critical Doping for the Onset of Fermi-Surface Reconstruction by Charge-Density-Wave Order in the Cuprate Superconductor $La_{2-x}Sr_xCuO_4$, Phys. Rev. X **6**, 021004 (2016).

[9] F. Laliberté, J. Chang, N. Doiron-Leyraud, E. Hassinger, R. Daou, M. Rondeau, B. Ramshaw, R. Liang, D. Bonn, W. Hardy *et al.*, Fermi-surface reconstruction by stripe order in cuprate superconductors, Nat. Commun. **2**, 432 (2011).

[10] B. Keimer, S. A. Kivelson, M. R. Norman, S. Uchida, and J. Zaanen, From quantum matter to high-temperature superconductivity in copper oxides, Nature (London) **518**, 179 (2015).

[11] T. J. Reber, X. Zhou, N. Plumb, S. Parham, J. Waugh, Y. Cao, Z. Sun, H. Li, Q. Wang, J. Wen *et al.*, A unified form of low-energy nodal electronic interactions in hole-doped cuprate superconductors, Nat. Commun. **10**, 5737 (2019).

[12] J. Ayres, M. Berben, M. Čulo, Y.-T. Hsu, E. van Heumen, Y. Huang, J. Zaanen, T. Kondo, T. Takeuchi, J. Cooper *et al.*, Incoherent transport across the strange-metal regime of overdoped cuprates, Nature (London) **595**, 661 (2021).

[13] A. Gourgout, G. Grissonnanche, F. Laliberté, A. Ataei, L. Chen, S. Verret, J.-S. Zhou, J. Mravlje, A. Georges, N. Doiron-Leyraud *et al.*, Seebeck Coefficient in a Cuprate Superconductor: Particle-Hole Asymmetry in the Strange Metal Phase and Fermi Surface Transformation in the Pseudogap Phase, Phys. Rev. X **12**, 011037 (2022).

[14] A. Georges and J. Mravlje, Skewed non-Fermi liquids and the Seebeck effect, Phys. Rev. Research **3**, 043132 (2021).

[15] P. Chaikin and T. Lubensky, *Principles of Condensed Matter Physics* (Cambridge University Press, Cambridge, 2000).

[16] L. V. Delacrétaz, B. Goutéraux, S. A. Hartnoll, and A. Karlsson, Bad metals from fluctuating density waves, SciPost Phys. **3**, 025 (2017).

[17] L. V. Delacrétaz, B. Goutéraux, S. A. Hartnoll, and A. Karlsson, Theory of hydrodynamic transport in fluctuating electronic charge density wave states, Phys. Rev. B **96**, 195128 (2017).

[18] L. V. Delacrétaz, B. Goutéraux, and V. Ziogas, Damping of Pseudo-Goldstone Fields, Phys. Rev. Lett. **128**, 141601 (2022).

[19] J. Armas, A. Jain, and R. Lier, Approximate symmetries, pseudo-Goldstones, and the second law of thermodynamics, arXiv:2112.14373.

[20] G. Grüner, The dynamics of charge-density waves, Rev. Mod. Phys. **60**, 1129 (1988).

[21] J. Zaanen, Y.-W. Sun, Y. Liu, and K. Schalm, *Holographic Duality in Condensed Matter Physics* (Cambridge University Press, Cambridge, 2015).

[22] S. A. Hartnoll, A. Lucas, and S. Sachdev, *Holographic Quantum Matter* (MIT Press, 2018).
[23] A. Amoretti, D. Areán, B. Goutéraux, and D. Musso, Effective holographic theory of charge density waves, Phys. Rev. D **97**, 086017 (2018).
[24] B. Goutéraux, N. Jokela, and A. Pönni, Incoherent conductivity of holographic charge density waves, J. High Energy Phys. 07 (2018) 004.
[25] A. Donos, J. P. Gauntlett, T. Griffin, and V. Ziogas, Incoherent transport for phases that spontaneously break translations, J. High Energy Phys. 04 (2018) 053.
[26] A. Amoretti, D. Areán, B. Goutéraux, and D. Musso, Diffusion and universal relaxation of holographic phonons, J. High Energy Phys. 10 (2019) 068.
[27] M. Baggioli and B. Goutéraux, Effective and holographic theories of strongly-correlated phases of matter with broken translations, arXiv:2203.03298.
[28] J. Armas and A. Jain, Viscoelastic hydrodynamics and holography, J. High Energy Phys. 01 (2020) 126.
[29] J. Armas and A. Jain, Hydrodynamics for charge density waves and their holographic duals, Phys. Rev. D **101**, 121901(R) (2020).
[30] H. Takagi, B. Batlogg, H. L. Kao, J. Kwo, R. J. Cava, J. J. Krajewski, and W. F. Peck, Jr., Systematic Evolution of Temperature-Dependent Resistivity in $La_{2-x}Sr_xCuO_4$, Phys. Rev. Lett. **69**, 2975 (1992).
[31] Y. Ando, G. S. Boebinger, A. Passner, T. Kimura, and K. Kishio, Logarithmic Divergence of both In-Plane and Out-of-Plane Normal-State Resistivities of Superconducting $La_{2-x}Sr_xCuO_4$ in the Zero-Temperature Limit, Phys. Rev. Lett. **75**, 4662 (1995).
[32] R. Arpaia, E. Andersson, E. Trabaldo, T. Bauch, and F. Lombardi, Probing the phase diagram of cuprates with $YBa_2Cu_3O_{7-\delta}$ thin films and nanowires, Phys. Rev. Materials **2**, 024804 (2018).
[33] F. Laliberté, W. Tabis, S. Badoux, B. Vignolle, D. Destraz, N. Momono, T. Kurosawa, K. Yamada, H. Takagi, N. Doiron-Leyraud *et al.*, Origin of the metal-to-insulator crossover in cuprate superconductors, arXiv:1606.04491.
[34] See Supplemental Material at http://link.aps.org/supplemental/10.1103/PhysRevB.106.L041118 for the details of the two holographic models considered, the details of our fitting procedure, and a set of checks on the AC results, as well as some additional results in a holographic model based on helical Bianchi VII geometry.
[35] S. de Haro, S. N. Solodukhin, and K. Skenderis, Holographic reconstruction of space-time and renormalization in the AdS/CFT correspondence, Commun. Math. Phys. **217**, 595 (2001).
[36] B. Withers, Black branes dual to striped phases, Classical Quantum Gravity **30**, 155025 (2013).
[37] A. Amoretti, D. Arean, D. K. Brattan, and N. Magnoli, Hydrodynamic magneto-transport in charge density wave states, J. High Energy Phys. 05 (2021) 027.
[38] A. Amoretti, D. Arean, D. K. Brattan, and L. Martinoia, Hydrodynamic magneto-transport in holographic charge density wave states, J. High Energy Phys. 11 (2021) 011.
[39] T. Andrade, M. Baggioli, and A. Krikun, Phase relaxation and pattern formation in holographic gapless charge density waves, J. High Energy Phys. 03 (2021) 292.
[40] P. Kovtun, Lectures on hydrodynamic fluctuations in relativistic theories, J. Phys. A: Math. Theor. **45**, 473001 (2012).
[41] M. Ammon, M. Baggioli, S. Gray, S. Grieninger, and A. Jain, On the hydrodynamic description of holographic viscoelastic models, Phys. Lett. B **808**, 135691 (2020).
[42] A. Amoretti, D. Areán, B. Goutéraux, and D. Musso, Universal Relaxation in a Holographic Metallic Density Wave Phase, Phys. Rev. Lett. **123**, 211602 (2019).
[43] R. A. Davison and B. Goutéraux, Dissecting holographic conductivities, J. High Energy Phys. 09 (2015) 090.
[44] R. A. Davison, B. Goutéraux, and S. A. Hartnoll, Incoherent transport in clean quantum critical metals, J. High Energy Phys. 10 (2015) 112.
[45] R. A. Davison, S. A. Gentle, and B. Goutéraux, Slow Relaxation and Diffusion in Holographic Quantum Critical Phases, Phys. Rev. Lett. **123**, 141601 (2019).
[46] R. A. Davison, S. A. Gentle, and B. Goutéraux, Impact of irrelevant deformations on thermodynamics and transport in holographic quantum critical states, Phys. Rev. D **100**, 086020 (2019).
[47] M. Ammon, M. Baggioli, and A. Jiménez-Alba, A unified description of translational symmetry breaking in holography, J. High Energy Phys. 09 (2019) 124.
[48] A. Donos, D. Martin, C. Pantelidou, and V. Ziogas, Incoherent hydrodynamics and density waves, Class. Quantum Grav. **37**, 045005 (2020).
[49] T. Andrade and A. Krikun, Coherent vs incoherent transport in holographic strange insulators, J. High Energy Phys. 05 (2019) 119.
[50] M. Baggioli, Homogeneous holographic viscoelastic models and quasicrystals, Phys. Rev. Research **2**, 022022(R) (2020).
[51] M. Baggioli and M. Landry, Effective field theory for quasicrystals and phasons dynamics, SciPost Phys. **9**, 062 (2020).
[52] C. P. Herzog, Lectures on holographic superfluidity and superconductivity, J. Phys. A: Math. Theor. **42**, 343001 (2009).
[53] S. A. Hartnoll, Lectures on holographic methods for condensed matter physics, Class. Quantum Grav. **26**, 224002 (2009).
[54] R. Flauger, E. Pajer, and S. Papanikolaou, A striped holographic superconductor, Phys. Rev. D **83**, 064009 (2011).
[55] Y. Liu, K. Schalm, Y.-W. Sun, and J. Zaanen, Lattice potentials and fermions in holographic non Fermi-liquids: Hybridizing local quantum criticality, J. High Energy Phys. 10 (2012) 036.
[56] G. T. Horowitz, J. E. Santos, and D. Tong, Optical conductivity with holographic lattices, J. High Energy Phys. 07 (2012) 168.
[57] G. T. Horowitz, J. E. Santos, and D. Tong, Further evidence for lattice-induced scaling, J. High Energy Phys. 11 (2012) 102.
[58] A. Donos and J. P. Gauntlett, The thermoelectric properties of inhomogeneous holographic lattices, J. High Energy Phys. 01 (2015) 035.
[59] M. Rangamani, M. Rozali, and D. Smyth, Spatial modulation and conductivities in effective holographic theories, J. High Energy Phys. 07 (2015) 024.
[60] B. W. Langley, G. Vanacore, and P. W. Phillips, Absence of power-law mid-infrared conductivity in gravitational crystals, J. High Energy Phys. 10 (2015) 163.
[61] A. Donos, Striped phases from holography, J. High Energy Phys. 05 (2013) 059.
[62] B. Withers, The moduli space of striped black branes, arXiv:1304.2011.

[63] A. Donos and J. P. Gauntlett, On the thermodynamics of periodic AdS black branes, J. High Energy Phys. 10 (2013) 038.

[64] A. Krikun, Holographic discommensurations, J. High Energy Phys. 12 (2018) 030.

[65] T. Andrade, A. Krikun, K. Schalm, and J. Zaanen, Doping the holographic Mott insulator, Nat. Phys. **14**, 1049 (2018).

[66] T. Andrade and A. Krikun, Commensurate lock-in in holographic non-homogeneous lattices, J. High Energy Phys. 03 (2017) 168.

[67] T. Andrade and B. Withers, A simple holographic model of momentum relaxation, J. High Energy Phys. 05 (2014) 101.

[68] A. Donos and J. P. Gauntlett, Holographic Q-lattices, J. High Energy Phys. 04 (2014) 040.

[69] M. Baggioli and O. Pujolas, Electron-Phonon Interactions, Metal-Insulator Transitions, and Holographic Massive Gravity, Phys. Rev. Lett. **114**, 251602 (2015).

[70] L. Alberte, M. Baggioli, A. Khmelnitsky, and O. Pujolas, Solid holography and massive gravity, J. High Energy Phys. 02 (2016) 114.

[71] M. Baggioli, K.-Y. Kim, L. Li, and W.-J. Li, Holographic Axion model: a simple gravitational tool for quantum matter, Sci. China: Phys., Mech. Astron. **64**, 270001 (2021).

[72] S. Nakamura, H. Ooguri, and C.-S. Park, Gravity dual of spatially modulated phase, Phys. Rev. D **81**, 044018 (2010).

[73] H. Ooguri and C.-S. Park, Holographic end-point of spatially modulated phase transition, Phys. Rev. D **82**, 126001 (2010).

[74] A. Donos and J. P. Gauntlett, Black holes dual to helical current phases, Phys. Rev. D **86**, 064010 (2012).

[75] A. Donos and S. A. Hartnoll, Interaction-driven localization in holography, Nat. Phys. **9**, 649 (2013).

[76] A. Donos, B. Goutéraux, and E. Kiritsis, Holographic metals and insulators with helical symmetry, J. High Energy Phys. 09 (2014) 038.

[77] A. Donos, J. P. Gauntlett, T. Griffin, N. Lohitsiri, and L. Melgar, Holographic DC conductivity and Onsager relations, J. High Energy Phys. 07 (2017) 006.

[78] A. Donos, J. P. Gauntlett, T. Griffin, and L. Melgar, DC conductivity of magnetised holographic matter, J. High Energy Phys. 01 (2016) 113.

[79] E. Banks, A. Donos, and J. P. Gauntlett, Thermoelectric DC conductivities and Stokes flows on black hole horizons, J. High Energy Phys. 10 (2015) 103.

[80] A. Donos and J. P. Gauntlett, Thermoelectric DC conductivities from black hole horizons, J. High Energy Phys. 11 (2014) 081.

[81] N. Iqbal and H. Liu, Universality of the hydrodynamic limit in AdS/CFT and the membrane paradigm, Phys. Rev. D **79**, 025023 (2009).

[82] A. Romero-Bermúdez, A. Krikun, K. Schalm, and J. Zaanen, Anomalous attenuation of plasmons in strange metals and holography, Phys. Rev. B **99**, 235149 (2019).

[83] F. Balm, A. Krikun, A. Romero-Bermúdez, K. Schalm, and J. Zaanen, Isolated zeros destroy Fermi surface in holographic models with a lattice, J. High Energy Phys. 01 (2020) 151.

[84] N. Gnezdilov, A. Krikun, K. Schalm, and J. Zaanen, Isolated zeros in the spectral function as signature of a quantum continuum, Phys. Rev. B **99**, 165149 (2019).

[85] S. Smit, E. Mauri, L. Bawden, F. Heringa, F. Gerritsen, E. van Heumen, Y. Huang, T. Kondo, T. Takeuchi, N. Hussey *et al.*, Momentum-dependent scaling exponents of nodal self-energies measured in strange metal cuprates and modelled using semi-holography, arXiv:2112.06576.